
System noise temperature measurement of EASIER/GIGADuck detectors

2

4

Abstract

The system noise temperature is a key characteristic of a radio detector such as EASIER's or GIGADuck's, since it directly relates to the sensitivity. Previous measurement of this characteristic for these antennas were done in laboratory by the CROME group and in situ by MIDAS group. We present a measurement of the noise temperature performed in situ for the GIGADuck detectors using the Sun's microwave flux as a calibration source. The sun's signal in the EASIER detectors being too small, we set up a dedicated measurement. We present in this note the methods to select and correct the monitoring data for GIGADuck and the method to retrieve the temperature for EASIER. We also detail the uncertainty calculation to finally obtain a noise temperature of $T_{sys} = ??? \pm$ for GIGADuck and $T_{sys} = ??? \pm$ for EASIER.

6

8

10

12

14

Introduction

16

EASIER and GIGADuck are two versions of a radio detector tuned in the C-band and installed on Auger SD station. They share the same basic design: the sensor is a feed horn antenna and it is connected to an amplifier. The Radio Frequency (RF) signal is then fed to a power detector which outputs a voltage proportional to the logarithm of the signal envelope. This voltage is in turn adapted to the SD front end input and is recorded as one of the 6 FE input channel (it replaces one of the PMT anode signal). EASIER was the original design, it uses commercial TV antenna pointing toward the zenith [?] and is implemented on 47 stations, while GIGADuck is installed on one hexagon and has the six surrounding detector pointing at a zenith angle of 20 degree and an azimuth of the central detector[?] direction. For such detector, a figure of merit of the sensitivity can be written as:

$$F = \frac{k_B T_{sys}}{A_{eff} \sqrt{\Delta t \Delta \nu}} \quad (1)$$

where k_B is the Boltzmann constant, T_{sys} is the system noise temperature, A_{eff} is the effective area of the antenna, and $\sqrt{\Delta t \Delta \nu}$ is the number of sample on can integrate on with $\Delta \nu$ the bandwidth and Δt the length of the expected signal.

The system noise temperature is thus a key parameter in the calibration of a radio detector. For EASIER and GIGADuck detectors, the noise comes from the thermal noise collected by the antenna, T_{ant} and the amplifier noise T_{elec} . The noise added by the element after the amplifier are reduced by the gain of the amplifier, around 60dB, and is thus negligible. The antenna temperature is obtained by integrating the sky and ground temperature (the brightness temperature) over 4π weighted by the antenna gain:

$$T_{ant} = \int_{\theta=0}^{\theta=\pi} \int_{\phi=0}^{\phi=2\pi} T_B G(\theta, \phi) d\theta d\phi \quad (2)$$

To measure the electronic temperature, one has to compare the output power when the system is irradiated with two known microwave sources. One reference is the antenna temperature computed in equation 2. The second reference can be the sun flux, it is used for the GIGADuck detector and detailed in section ??, however due to a smaller antenna gain, we can't use the sun signal for EASIER, we then use the antenna temperature when the antenna points toward the ground, this method is detailed in ??.

1 Expected signal from the sun flux

44

We present in this section the calculation of the expected signal from the solar flux. The main ingredients are:

46

- the sun flux (the sun flux varies with time)
- the sun path with respect to the antenna depending on the time of the year
- the antenna pattern

48

Given these ingredients one can estimate the additional power at the sun passage:

50

$$P_{sun}(t) = \frac{1}{2} F_{sun} A_{eff}(\theta(t), \phi(t)) [W/Hz] \quad (3)$$

where the factor $\frac{1}{2}$ comes from the polarization selection of the antenna.

52

1.1 Sun flux

The sun flux is measured by dedicated observatories around the world[?, ?] at several frequencies. We use the flux at 2.8GHz (so called F107) whis is widely measured. In order to extrapolate to the frequency band we are interested we use a paramterization. In the microwave frequency range, the sun flux has two main contributions [?]: a quiet sun component (or background component) with a constant intensity and a frequency dependence as:

$$S_q [SFU] = 26.4 + 12.4 \nu + 1.11 \nu^2 \text{ for } (1 < \nu(\text{GHz}) < 20) \quad (4)$$

a second contribution, the so called slowly varying component, its spectrum is parameterised as:

$$S_v [SFU] = \frac{0.64(F10.7 - 70)f^{0.4}}{1 + 1.56(\ln(f / 2.9))^2} \quad (5)$$

These spectra are shown in the figure 1 An example of the sun flux at 10.7cm is shown in the

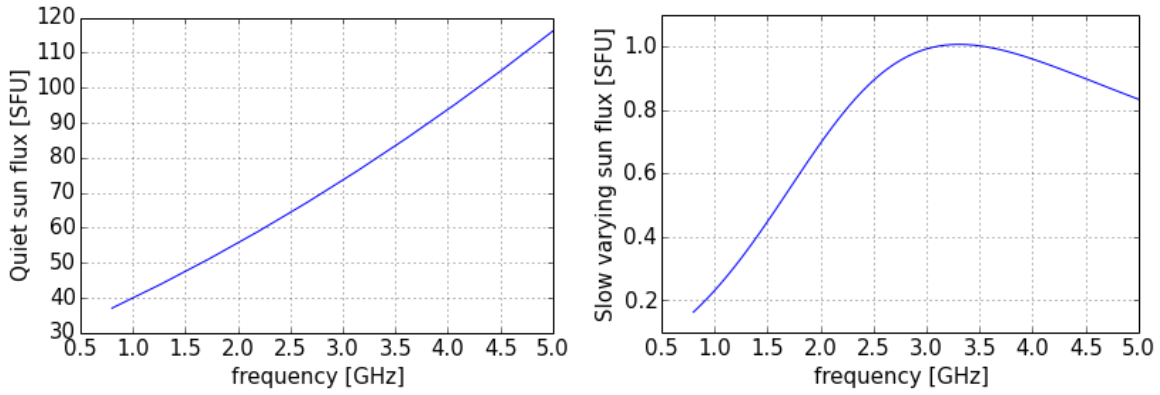


Figure 1 Left: quiet sun spectrum, Right: varying component spectrum

Figure 2. One can notice the quasi monthly modulation that can be of the order of 30-40% and justify the use of a daily measurement instead of a month or a year average.

1.2 the sun transit

The other ingredient, the sun transit on the sky of Malargüe is found using the code Sun Position Algorithm (SPA) [1]. Examples of the path during the year are shown in polar coordinate where the radius is the zenith angle and the angle is the azimuth (90 degree is the north).

1.3 the antenna pattern

The last ingredient is the effective area of the antenna in the direction of the sun position. The angular gain, directly related to the effective area, was measured in anechoic chamber for the EASIER antennas [?], for the GIGADuck detectors we rely on pattern simulation performed with HFSS software. Note that the antenna geometry is rather simple (horn antenna) so that the simulations for our purpose is reliable. The gain explored for an EASIER or a GIGADuck antenna (the vertical one) is shown in the figure 3 (middle plots) next to the sun

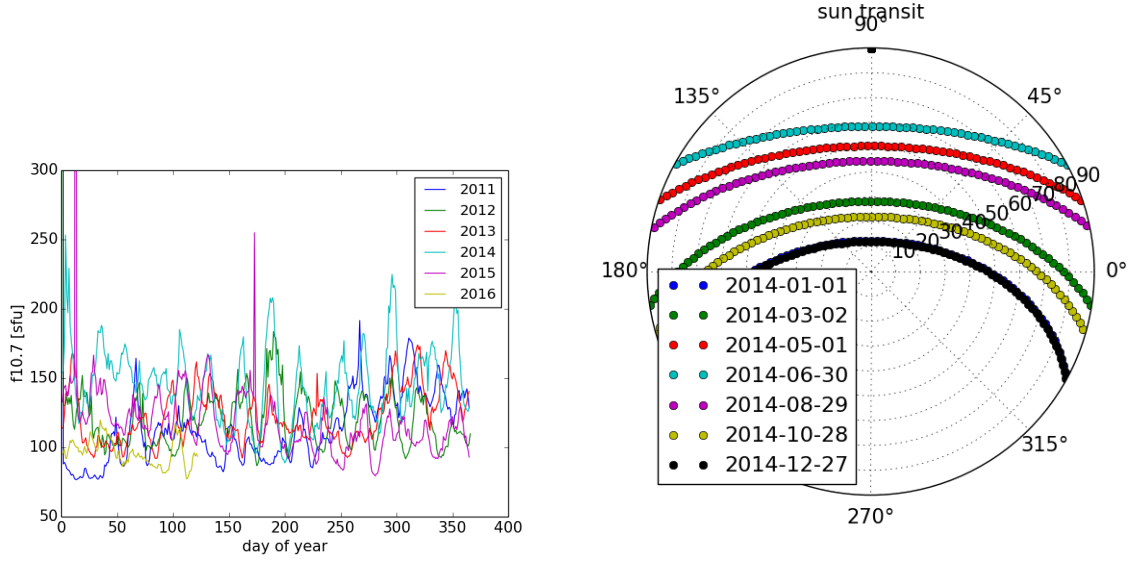


Figure 2 Left: f107 from 2011 to 2015. Right: sun transit along the year

path during one day. One can directly compare the gain of the two detectors. The right 78
hand side plot of the same figure, show the expected signal in ADC counts for three assumed 80
system temperature. It shows that even for a small system temperature, the baseline changes 80
are small in the case of EASIER. For GIGADuck, one can expect around 20ADC count for a
system noise temperature of 50 K. The expected signal in EASIER is small, and other effects 82
than the sun can affect the baseline with such amplitude. We will only use the sun for the
GIGADuck antennas. EASIER detector will be calibrated with another method described in 84
section??.

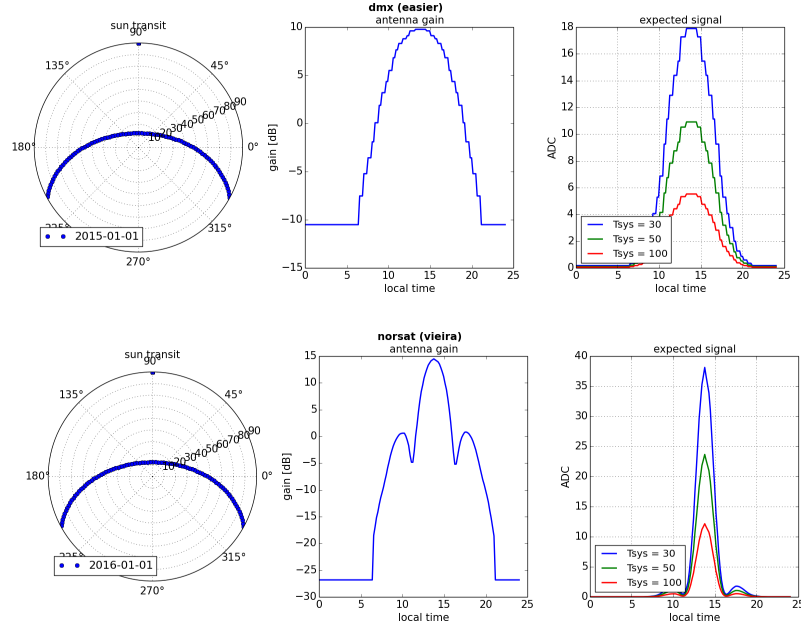


Figure 3 Expected signal from the sun for the EASIER detector (top) and GIGADuck (bottom). The three pannels indicate the from left to right: the sun path in the sky, the gain in the sun's direction during the day, the expected signal in ADC count for three different system temperatures.

2.1 Data selection

The radio baseline we observe is a results of several known and unknown effects. A daily modulation is due to the temperature and will be corrected for in section 2.2. Humidity can affect a lot the baseline, but the parameterization is more difficult. We also notice some large change of the baseline that are likely to be due to storm. We present in this section the cut we operate to clean the data and keep the period when the baseline is mainly affected by the temperature.

In principle we could make cuts on humidity value, but the monitoring information is not always present. We operate the selection only the shape of the radio baseline and select the days when the variations are smooth. The figure 4 shows the day selected for the station Popey. For instance, the period around the 25th of March was certainly a period of rain, and the baseline of Chape and Popey is affected, thus this period is removed from the dataset. (The date are also reported in the appendix)

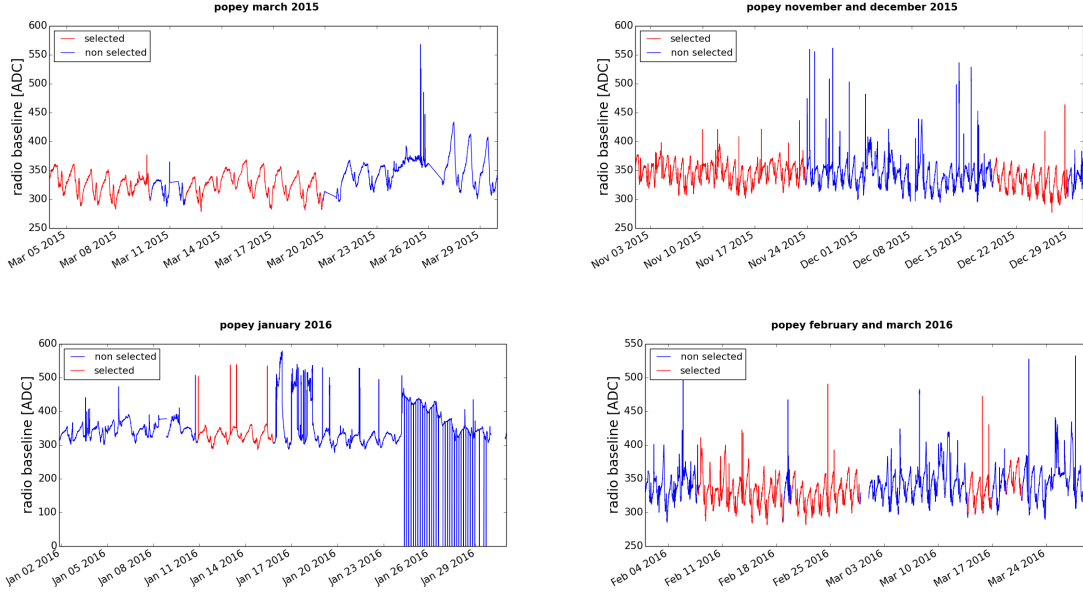


Figure 4 Radio baseline for four different periods for Popey station (id=385). In red are the periods kept for the sun transit analysis based on the shape.

2.2 Temperature dependence

100

The next step is to correct from the effect of temperature. First of all we remove the time of the day when the sun is expected (this time depends on the station because they point toward 102 different azimuth). The raw plot of the baseline vs temperature is shown on the figure 5. For Chape we notice two separated populations. This is due to the fact that we have sometimes 104 a jump of the baseline. To circumvent this effect, we reference our data to the daily average (see Figure ??). We parameterize only the variation of the radio baseline with the variation 106 of the temperature:

- Chape: $\text{ADC} - \langle \text{ADC} \rangle = -2.93(T - \langle T \rangle)$ 108
- Popey: $\text{ADC} - \langle \text{ADC} \rangle = -3.67(T - \langle T \rangle)$

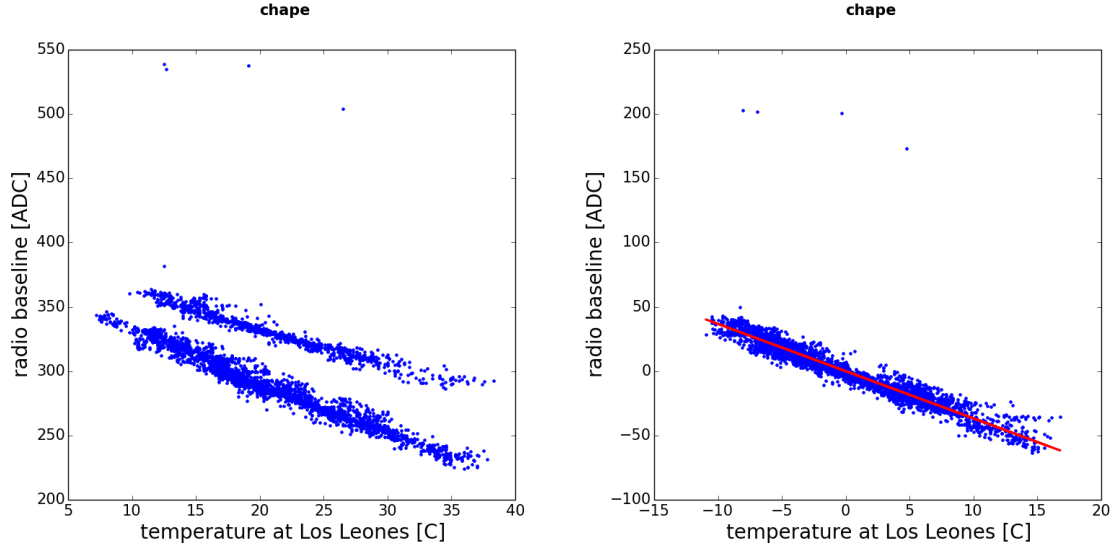


Figure 5 Selected period in red for Popey

2.3 Fit of the sun signal

110

The temperature correction removes the dominant modulation. The sun signal is then fitted with a Gaussian function. Example of such a fit is shown in the Figure 6. A last selection is 112 done here on the fit output parameter. We remove the day when the fit value of the time of maximum is more than 1 hour away from the expected one and the sigma of the gaussian is 114 less than 20 minutes or more that 1.5 hour.

2.4 Temperature measurement uncertainties

116

The formula we use to retrieve the temperature is:

$$T_{\text{by's}}(F_{\text{sun}}, A_{\text{eff}}, \Delta P) = \frac{\frac{1}{2} F_{\text{sun}} A_{\text{eff}}}{10^{\frac{\Delta P}{10}} - 1} \quad (6) \quad 118$$

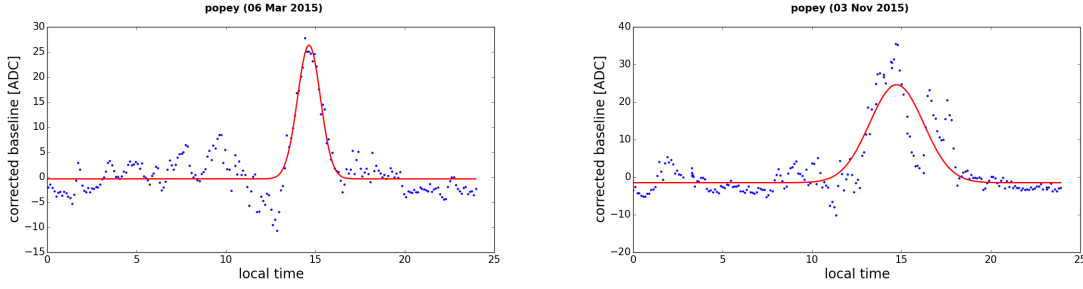


Figure 6 Left: good fit example. Right: bad fit

Where F_{sun} is the sun flux measured by other observatory, A_{eff} is the effective area in the sun's direction, ΔP is the power difference in dB (with $1\text{dB} = 50$ ADC count) and the factor $\frac{1}{2}$ is the polarization factor (we only observe one of the two polarizations). The uncertainties on T_{sys} is then:

$$\sigma_{T_{\text{sys}}}^2 = \frac{T_{\text{sys}}^2}{F_{\text{sun}}^2} \sigma_{F_{\text{sun}}}^2 + \frac{T_{\text{sys}}^2}{A_{\text{eff}}^2} \sigma_{A_{\text{eff}}}^2 + T_{\text{sys}}^2 \left(\frac{\frac{\ln(10)}{10} 10^{\frac{\Delta P}{10}}}{10^{\frac{\Delta P}{10}} - 1} \right)^2 \sigma_{\Delta P}^2 \quad (7)$$

2.4.1 Sun flux uncertainties

Here we check the precision we have on the sun flux. Up to now, we get data at 2.8GHz (commonly called f107) and extrapolate the value at 3.8GHz with parameterisation of the quiet sun and the slowly varying sun. We can compare our results with the Nobeyama observatory data, which collects data on the sun flux at 2 and 4 GHz (we don't use their data yet because they don't release them on the web). The figure 7 shows different fluxes:

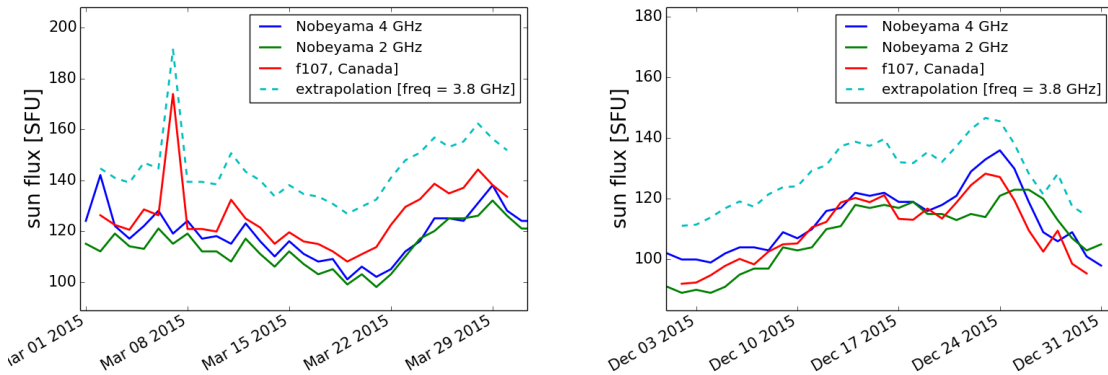


Figure 7 sun flux for at different frequencies

The value reported on the plots for the Nobeyama observatory are taken from what is displayed on their daily curves. I don't really know if this is an average or the minimum value. In any case, the values at 2 and 4 GHz are lower than what is measured at the Canadian site [2, ?] by around 20%. Since I am still not sure of the meaning of the value for

the Nobeyama data, I will account for an uncertainty of 20% in the temperature calculation 134 (this has to be improved either by taking the data of Nobeyama or by determining a precise uncertainty.). This number of 20% corresponds also to what is given in the 136 website [3] where we found the parameterisation.

2.4.2 Effective area uncertainties

138

We do have also some uncertainties on the effective area, be it because of the pointing direction or our knowledge of the gain. We estimate the possible shift in pointing to 2° . The resulting 140 uncertainty on the gain depends on the zenith angle at the sun maximum. The figure 8 shows the effective area and a Gaussian fit as a function of the zenith angle and the uncertainties 142 on the effective area based of the Gaussian fit.

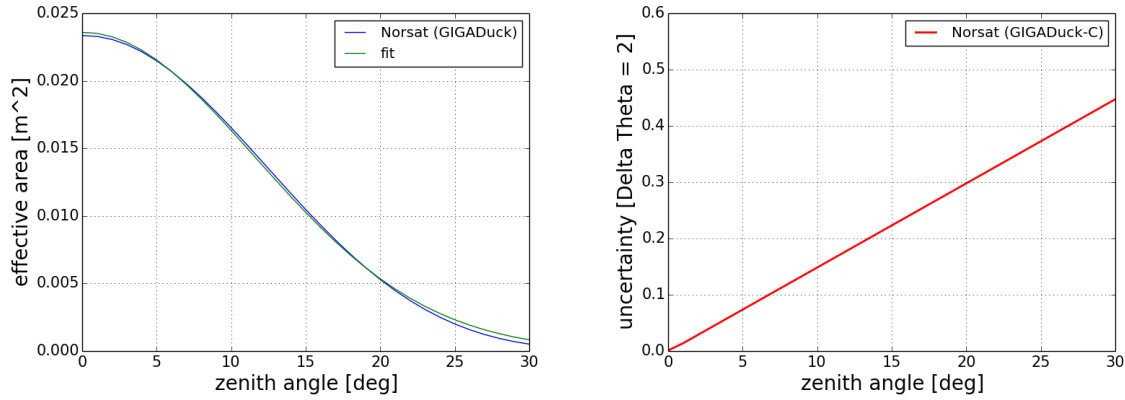


Figure 8 Effective area of the AInfo antenna from HFSS simulation (blue), Gaussian fit (green). Right: relative uncertainty on the effective area

We perform the temperature measurement only during the months when a significant 144 signal from the sun is expected, that means when it is high in the sky. The zenith angle at which the sun signal is maximum (in the simulation) is shown in the figure 9 for three 146 antenna: Vieira the central detector that points up to the zenith, Chape and Orteguina (see figure ?? for their field of view). The angle at which the sun is observed when the signal is 148 maximum is below 10° for Chape but around 15 to 20° in March for Vieira or Orteguina.

2.4.3 Uncertainty on ΔP

150

The uncertainty on the measured power induced by the sun flux comes from our ability to measure a variation of baseline on an hour time scale. The process to estimate this variation, 152 summed up in section ??, is based on a fit of the sun bump with a Gaussian function and the background with a second order polynomials. There aren't actually any justification for the 154 background fit. To estimate the error on the ΔADC we make, we change the fitting method and see how the results change. The figure ?? shows the results of ΔADC as a function of 156 the date when the baseline is either fitted with a constant and a Gaussian or with a second order polynomial and a constant, on the right side is shown the corresponding histogram of 158 the difference of the two methods.

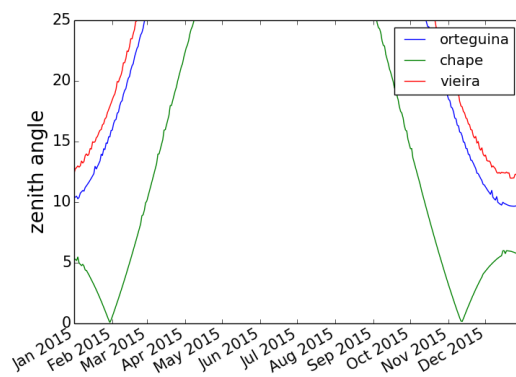


Figure 9 Zenith angle when the sun signal is maximum as a function of the date

References 160

- [1] I. Reda and A. Andreas, *Solar position algorithm for solar radiation applications*, Solar Energy **76** (2004) 577–589. 162
- [2] <http://omniweb.gsfc.nasa.gov/form/dx1.html>.
- [3] <http://www.spaceacademy.net.au/spacelink/solrfi/solrfi.htm>. 164